Emerging pathways in electrical, magnetic and thermoelectric performance of different concentration of iron doped cobalt oxide nanoparticles

Numan Abbas [a], Jian-Min Zhang [a,*], Abdul Rehman Gill [b], Muhammad Zeeshan Asad [b], Arslan Mahmood [c], Muhammad Ikram [a], Sohail Ahmad [d], Muhammad Atif [e], Muhammad Jehanzaib Aslam [f,*]

[a] College of Physics and Information Technology, Shaanxi Normal University, Xian 710119, Shaanxi, PR China
[b] Department of Physics, University of Agriculture Faisalabad, Pakistan
[c] Department of Physics, Government College University Faisalabad (GCUF), Allama Iqbal Road, Faisalabad 38000, Pakistan
[d] Institude of Physics, Bahauddin Zakariya University, Multan 60000, Pakistan
[e] Department of Physics and Astronomy, College of Science, King Saud University Riyadh 11451, Saudi Arabia
[f] Department of Physics, Florida A&M University, Tallahassee, Florida 32307, USA

ARTICLE INFO

ABSTRACT

Current study was reported that to tune the magnetic, electrical and thermoelectric properties of Co_3O_4NPs by using different concentration of iron (0, 3 and 5 wt%). The Fe doped Co_3O_4 NPs were synthesized by using co-precipitation method. The XRD was use to identify the cubic spinel structure and crystallite size range from 15 to 24 nm. The porous like surface morphology changed into tiny spherical grain with 5 % Fe doped Co_3O_4 NPs was observed via SEM micrographs. After that the presence of CoO, FeO, CO, CO_2 and OH was identify with the help of FTIR analysis. In addition, VSM analysis shows that magnetization increase (20.918 E-3 to 73.843E-3 emu), corecivity, retentivity and ferromagnetic behavior decreased by increasing Fe concentration in Co_3O_4 NPs. Further, two probe method was used to examine the relation between resistivity and conductivity. It was observed that the resistivity decreases (9×10^3 to 3×10^3 Ω m) and conductivity increased (1.1×10^{-4} to 3.3×10^{-4} $Ω^{-1}m^{-1}$) upto significant level. Finally, thermoelectric property was identified to calculate seebeck coefficient and power factor. Thermoelectric result shows that due to increase the distance between source and substrate then seebeck coefficient and power factor increased. The seebeck coefficient values indicated that due to decrease the resistivity the carrier concentration increase upto significant value at optimum temperature. The synthesized nano-material will be suitable for spintronic devices, supercapacitor for electrode material and temperature sensors.

1. Introduction

Globally increased the energy crisis day by day and these crises was controlled by improve the physicochemical, magnetic, electrical and thermoelectric properties of different transition metal oxide NPs (Sangaiya & Jayaprakash, 2018). These properties also tune by using different doping, functionalizing and stabilizing agents (Xiao et al., 2019). Recently, transition metal oxides attract the attention of researches because these metals were played the central role in energy storage devices, communication purpose, reduce eddy current, data storage devices and biomedical applications (Sun et al., 2014; Yeoh et al., 2018; Mahmood et al., 2023). Huge number of metal oxide NPs

such as Fe_2O_3, NiO, ZnO, TiO_2, V_2O_3, Sc_2O_3 and Co_3O_4 was preferable due to magnetic, electrical and thermoelectric applications point of view. Here, Co_3O_4 NPs mostly used as a p-type semiconductor, solar absorber, magnetic material, gas sensors, dielectric material and energy storage devices (Pagar et al., 2019). The properties of metal oxide NPs depend upon shape, particle size and surface morphology. Morphology and particles size was controlled by controlling the temperature and pH during synthesis process (Callegari et al., 2003).Fig. 1.

The different synthesis methods was preferred to synthesized metal base oxide, sulfide and nitride NPs such as sol–gel, hydrothermal, co-precipitation, auto-combustion, autoclave method and solution evaporation method (Li et al., 2014; Munir et al., 2023; Munir et al., 2021).
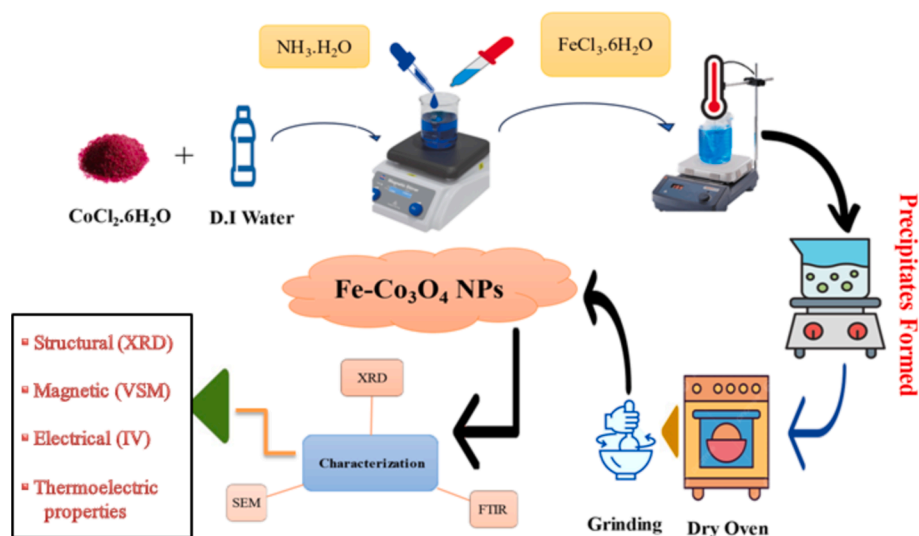

Fig. 1. Synthesis process of Fe doped Co$_3$O$_4$-NPs.

The preference of these methods depends upon the low cost, environment friendly and less time consuming. Ankita et al. (2024) reported that magnetic and photocatalytic was increased by doping europium in cerium oxide NPs (Ankita et al., 2024). Munir et al. (2021) reported that to enhance the optical and electrical properties by using different concentration of Cu doped in ZnO-NPs. Jiangjiang et al. (2024) provided the information about the thermoelectric properties enhance upto significant level by doing Aluminum oxide into indium oxide NPs (Jiangjiang et al. 2024). Yang et al. (2024) provided the information about electrocatalytic oxygen evolution by using metal doped in cobalt oxide NPs (Co$_3$O$_4$) (Yang et al., 2024). Mostly, previous study shows that by using different metal doping agents to enhance the electrochemical properties of Co$_3$O$_4$ thin film (Behzad & Ghodsi, 2016). Only, few study provided the information about Fe doped Co$_3$O$_4$ NPs used for biomedical application for the treatment of cancer and enhance the anticancer activity (Jincy & Meena, 2022).

Present research work was related to synthesis of bare and Fe doped Co$_3$O$_4$ NPs by varying concentration of Fe (0, 3 and 5 %) via co-precipitation method. After that the prepared powder form of all samples were characterized by using XRD for structural information, SEM was used to investigate surface morphology and rotational and vibrational modes was appeared in spectrum of Fe doped Co$_3$O$_4$ NPs was observed with FTIR analysis. The magnetic behavior of all prepared

samples was calculated with VSM analysis. The two probe method was used to draw the relation between resistivity and conductivity. At the end thermoelectric property was observed to investigate the seebeck coefficient and power factor Fe doped Co$_3$O$_4$ NPs.

2. Experimental procedure

2.1. Precursors

All precursors of analytical grade such as cobalt chloride hexahydrate (CoCl$_2$·6H$_2$O) (99.9 %), ferric chloride hexahydrate (FeCl$_3$·6H$_2$O) (98 %) and ammonia solution (NH$_4$OH) (99.2 %) were purchased form Sigma-Aldrich. All chemicals were used for the preparation of Fe incorporation in Co$_3$O$_4$ NPs. In addition, distilled water and ethanol also used for synthesis process and washing purpose were purchased from local market.

2.2. Synthesis methodology of Co$_3$O$_4$-NPs

The cobalt oxide (Co$_3$O$_4$) NPs was synthesized via co-precipitation. For this purpose cobalt chloride hexahydrate (1.18 g) was added into 50 mL distilled water and then stirring on magnetic stirrer to obtained mixture of cobalt oxide solution at room temperature for 30 min. After that to adjust the required pH upto 11 by adding NH$_4$OH (32 %) solutions drop by drop in cobalt mixture. Then the resulting solution was stirred and heated upto 80 °C for two hours. Then prepared precipitate was filtered and washed for three to four time with water and ethanol. Finally, prepared precipitate dried in laboratory oven at 150 °C for three hours. The prepared powder was grinded with mortar and pestle and then calcination was completed in tube furnace for two hours at 400 °C.

2.3. Synthesis of iron doped cobalt oxide-NPs

Same procedure was used to prepared cobalt hydroxide solution by adding 3 wt% iron solution and continuous stirring for 30 min at 100 °C. Similar process was used by using 5 wt% iron doped in Co$_3$O$_4$ NPs. Then prepared Fe doped Co$_3$O$_4$ precipitate filter, dry and calcinated by using same process was discussed earlier.

2.4. Characterization techniques

The structural analysis was completed with XRD (Bruker D8 Advanced) by using Cu$_\alpha$ (1.54 nm) wavelength. Surface morphology of prepared nanoparticles was investigated by using cube emcraft SEM.
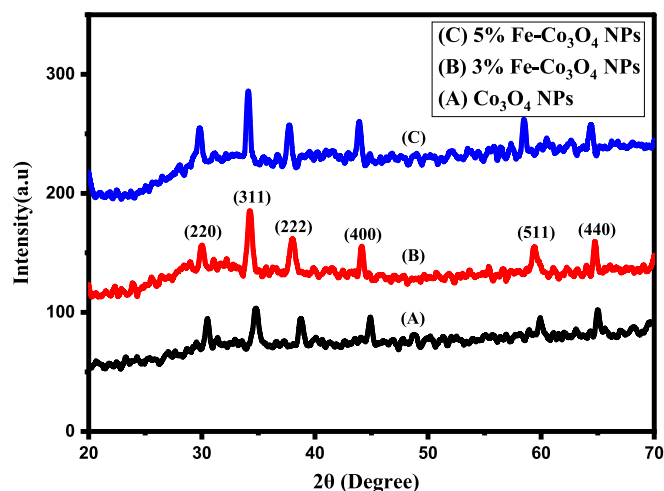

Fig. 2. XRD spectrum of Fe-doped cobalt oxide NPs.

Table 1
Shows crystallite size of fe doped co₃o₄-NPs.

Nanoparticles	Crystallite size (nm)
Co_3O_4 NPs	15.56
3 % Fe dopedCo₃O₄ NPs	17.47
5 % Fe dopedCo₃O₄ NPs	23.5

After that to observe the vibrational and rotational modes was appeared on spectrum was examined via FTIR "Bruker spectrometer". The magnetic property of prepared samples was examined with the help of VSM (Lakshore-7407 model). Electrical behavior of synthesized NPs was calculated two probe method with model Electric meter Keithley (2401) and also calculated the resistivity and conductivity. Finally, homemade thermoelectric measurement system used to calculate thermoelectric behavior of Fe doped Co_3O_4-NPs.

3. Results and discussion

3.1. Structural analysis

The structural analysis which includes structure and crystalline phase of pure and Fe doped Co_3O_4-NPs was completed with XRD analysis. Fig. 2 represents the XRD spectrums of pure and Fe-doped Co_3O_4-NPs. While as XRD spectrum of Fe-doped Co_3O_4-NPs of all samples was obtained by adjusting different vale of 2θ lies in the range from 20° to 70°. Further, appeared spectrum of all samples exhibit similar peaks corresponding to few indices like (220), (311), (400), (511) and (440)
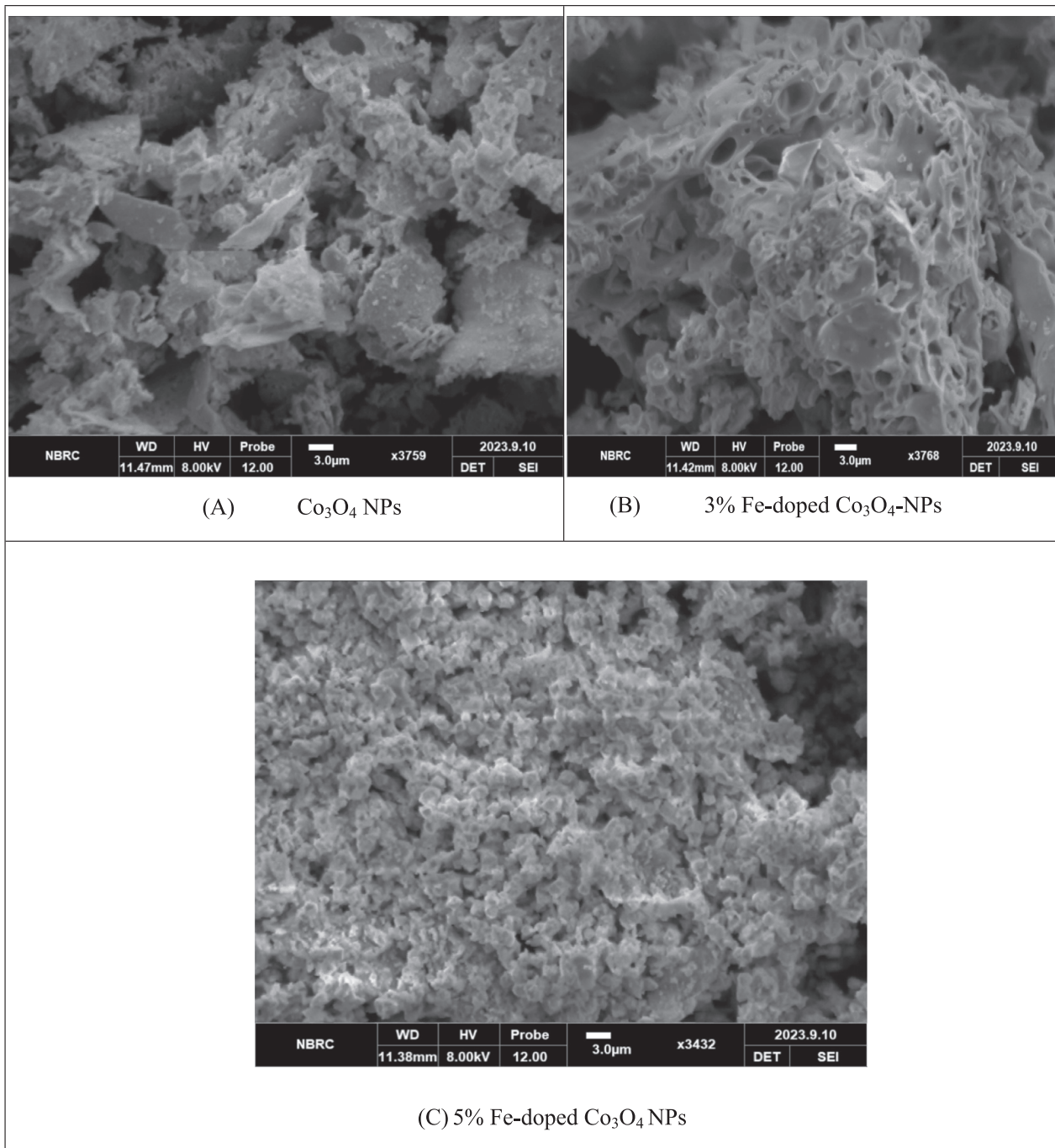

(A) Co_3O_4 NPs

(B)   3% Fe-doped Co_3O_4-NPs

(C) 5% Fe-doped Co_3O_4 NPs

Fig. 3. Surface morphology of Fe-doped Co_3O_4 NPs.

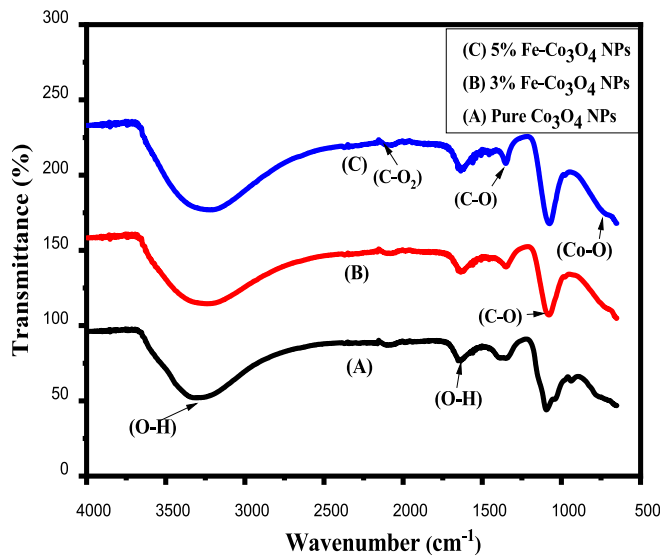**Fig. 4.** FTIR spectrum of Fe-doped Co_3O_4 NPs.

Fig. 5. M–H curve of Fe doped Co_3O_4-NPs.

compared with JCPDS no: 042:1467 (Karthikeyan et al., 2023; Alem et al., 2023). In addition, spinel cubic structure was appeared at preferable reflection plane (311). The spectrum was appeared by doping Fe in Co_3O_4 clearly indicated that the intensity of peaks increase by doping element and peaks shifted toward shorter wavelength (Guragain *et al.*, 2019). The peaks shifting due to crystal lattice distortion, it means that atomic radius of Fe^{3+} (6.4 nm) replacing Co^{3+} (6.2 nm) in Co_3O_4 NPs lattice. The peaks become intense and more sharp as the doping increase and crystal size increased upto significant value with the higher concentration of Fe doped Co_3O_4-NPs. The sharpness shows that crystalline nature improved with doping atom and crystallite size was calculated via Scherrer formula (1) written in Table 1. There was no extra peak appeared in doped spectrum, it means that Fe successfully doped in Co_3O_4NPs lattice.

$$D = \frac{k\lambda}{\beta cos\theta} \tag{1}$$

3.2. Morphological analysis

The SEM was used to collect the information about surface morphology of Fe-doped Co_3O_4 NPs. Fig. 3 represents the micrographs of Fe-doped Co_3O_4 NPs (A) Co_3O_4 NPs (B) 3 wt% Fe-doped Co_3O_4 NPs (C) 5 wt% Fe-doped Co_3O_4 NPs. All the micrographs were collected same resolution but in case of pure Co_3O_4 NPs micrograph shows irregular small and large grain was observed (Hafeez et al., 2020). It was examined that by using the 3 % iron doping agent in Co_3O_4 NPs shows porous like surface was appeared throughout the micrograph. Furthermore, the 3 % iron doped image also shows the agglomeration of Co_3O_4 NPs increase by using iron doping agent (Li et al., 2020). But in case of 5 % Fe doped Co_3O_4 NPs have uniformly distributed with tiny spherical structure with numerous porous throughout the surface. It has been demonstrated that presence of pores reduce and agglomeration increase by increasing doping atom (Gahrouei et al., 2020). The present micrographs expressed that the grain size was decreased and uniformity in surface morphology increase in of Co_3O_4 NPs by increasing Fe concentration.

3.3. FTIR analysis

The FTIR spectrums were obtained to investigation the presence of vibrational and rotational modes in Fe doped Co_3O_4-NPs. Fig. 4 shows the FTIR spectrum of Fe-doped Co_3O_4 NPs. The FTIR analysis was
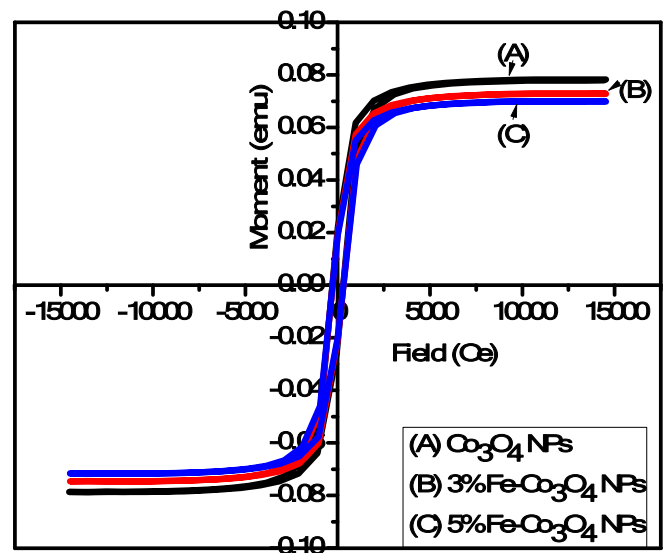
performed by using powder form samples were scanned from 650 to 4000 cm^{-1} wavenumber (Manickam et al., 2017). The spectrum provided numerous bonds at different wavenumber like as wavenumber of 680 cm^{-1} was represented of stretching vibrations of Co-O bonds in case of pure Co_3O_4 NPs. In addition, by adding doping agent in Co_3O_4 NPs then stretching peak shifted towards smaller wavenumber (Soni et al., 2023). As we know that the inverse relation between mass and vibrational frequency and then due to enhance the vibrational frequency of Fe^{3+} with small atomic weight of Fe (55.8 u) replace with Co (58.9 u) ion. Additionally, few extra peaks was observed at 1075 cm^{-1} and 1349 cm^{-1} was associated with the C-O band and the wavenumber 3313 and 1636 cm^{-1} were shows the presence O–H vibrational modes due to the presence of water concentration in sample. Further, at 2300 cm^{-1} represents the presence of carbon dioxide, carbon mono-oxide and the addition of CO and CO_2 through atmosphere during synthesis process (Zuhra et al., 2023).

3.4. VSM analysis

The magnetic property of different concentration of Fe-doped Co_3O_4 NPs was examined via VSM analysis. Fig. 5 shows the hysteresis loop of Fe-doped Co_3O_4 NPs. All the samples shows hysteresis loop was measured at room temperature which indicate ferromagnetic behavior was dominant in Fe-doped Co_3O_4 NPs (Stella et al., 2015) The sample (A) Co_3O_4 NPs express intrinsic coercivity (Hci = 284.80 Oe), magnetization (Ms = 0.12465 emu) and retentivity (Mr = 20.918E-3 emu). But in case of 3 % Fe-doped Co_3O_4 NPs sample shows intrinsic coercivity (Hci = 230.29 Oe), magnetization (Ms = 73.843E-3 emu) and retentivity (Mr = 18.064E-3 emu). Similar behavior was observed by increasing the iron doping concentration in Co_3O_4 NPs. The measured value of M–H loop shows that by increasing iron doping concentration in Co_3O_4 NPs then magnetization power increase upto significant value but coercivity and retentivity decrease respectively. It was also observed that the ferromagnetic behaviour reduce by increasing the Fe concentration in Co_3O_4-NPs. Zhang and group fellows also reported that the iron doped Co_3O_4 NPs shows less ferromagnetic behavior at low temperature (Zhang et al., 2013).

3.5. I-V analysis

The electrical behavior of different concentration (0, 3 and 5 %) Fe-doped Co_3O_4 NPs was investigated by using current voltage relation. Fig. 6 indicates the relation between conductivity and resistivity. The
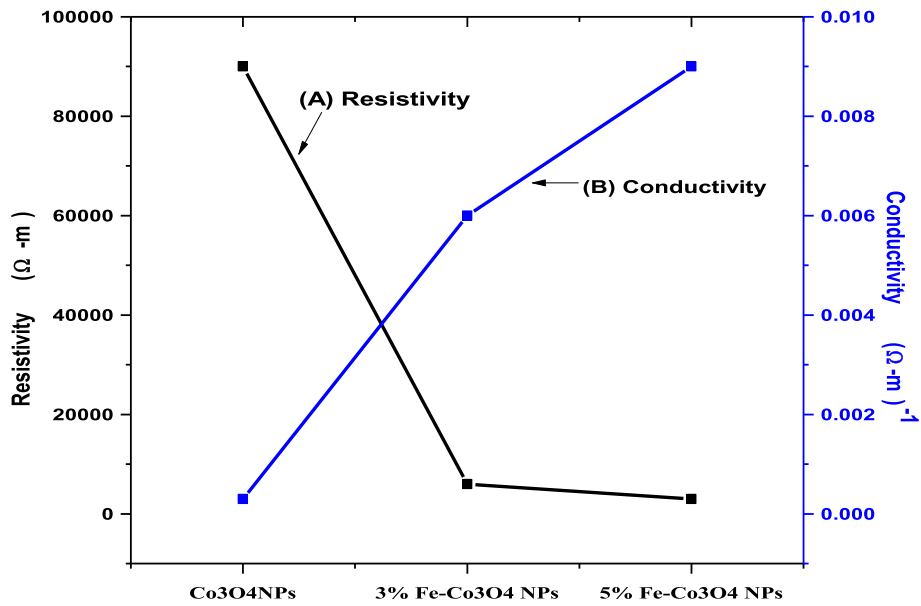
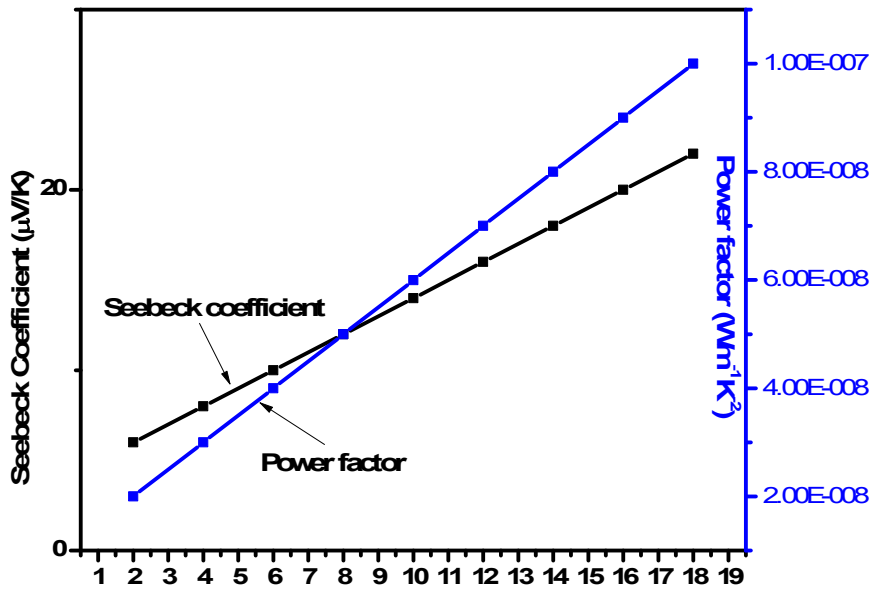**Fig. 6.** Conductivity and resistivity of Fe-doped Co_3O_4 NPs.

Fig. 7. Relation between seebeck coefficient and power factor.

resistivity of all samples were calculated by using equation (2) and resistivity of Co_3O_4NPs was calculated (9.00E + 3). It was examined that the resistivity of Co_3O_4 NPs decreases by increasing temperature (Bhargava et al., 2018). But current study was indicated that the variation of resistivity depends upon the Fe concentration doped Co_3O_4 NPs (3.00E + 3). The reciprocal of resistivity known as conductivity and conductivity of all samples was measured by taking the reciprocal of resistivity measured values. The Fig. 6 shows that the resistivity of Co_3O_4 NPs was decreased by increasing iron concentration and conductivity increased (Mahmood et al., 2022). Due to decrease the resistivity and increase conductivity of Fe doped Co_3O_4 NPs shows that the material is suitable for electrical devices and for supercapacitor electrode.

$$\rho = \frac{RA}{L} \tag{2}$$

3.6. Seebeck coefficient

The thermoelectric property depends upon the calculated value of seebeck coefficient of Fe doped Co_3O_4 NPs by using different concentration of Fe (0, 3 and 5 %). Fig. 7 describe the relation between seebeck coefficient and power factor. The equation (3) was used to calculate the variation values of seebeck coefficient of Fe doped Co_3O_4 NPs.

$$S = -(k/e)[\ln(N_v/n)+A] \tag{3}$$

Different parameter was used in equation (3) such as "k" represent Boltzmann constant, presence of charge carriers express by "n" and "A" shows the transport constant, its value exist in between 0 and 2 (Abbas et al., 2024). Fig. 7 represents the distance between source and substrate along horizontal axis in both vertical axes shows seebeck and power factor. It was clearly indicated that if the distance increase then seebeck and power factor increase due of greater concentration of charge carriers (Ibrahim et al., 2018). The electrical result shows that resistivity

decrease then charge carrier have greater ability to move quickly without energy loss. The current analysis also shows that by increasing the temperature upto optimum value then charge carrier response quickly. According to our review the thermoelectric behavior of Fe doped Co_3O_4 NPs was reported first time.

4. Conclusion

The iron doped Co_3O_4 nanoparticles were prepared via co-precipitation method. The presence of cubic spinel structure and variation of crystallite size in between 15 to 24 nm was calculated with the help of XRD analysis. The measured value of crystallite size shows that the crystallite size increased upto significant value by increasing Fe concentration in cobalt oxide. While as SEM analysis shows that porous like surface morphology changed into small uniform sphere was observed in 5 % Fe doped Co_3O_5 NPs micrograph. After that the presence of Fe in Co_3O_4 NPs and also observe the presence of functional groups attached with spectrum was investigated with FTIR analysis. The VSM analysis shows that magnetization power increase by increasing Fe but ferromagnetic behavior decreased. Finally, I-V analysis shows that by increasing iron concentration in Co_3O_4 NPs then conductivity increased and resistivity decreased. Due to decrease resistivity the charge carrier concentration increases at optimum value of temperature. It means that the prepared material will be most suitable for energy storage device, supercapacitor electrode fabrication and reduce the eddy loss.

CRediT authorship contribution statement

Numan Abbas: Writing – original draft. **Jian-Min Zhang:** . **Abdul Rehman Gill:** Formal analysis. **Muhammad Zeeshan Asad:** Formal analysis. **Arslan Mahmood:** . **Muhammad Ikram:** Formal analysis. **Sohail Ahmad:** Formal analysis. **Muhammad Atif:** Formal analysis. **Muhammad Jahanzab Aslam:** Investigation, Formal analysis.

Declaration of competing interest

The authors declare that they have no known competing financial interests or personal relationships that could have appeared to influence the work reported in this paper.

Acknowledgments

Appendix A. Supplementary data

Supplementary data to this article can be found online at https://doi.org/10.1016/j.jksus.2024.103565.

References

Abbas, N., Zhang, J.M., Ikram, M., Ibrahim, A.A., Nazir, S., Ali, I., Akhtar, H., 2024. Investigation of structural, electrical and thermoelectric properties of cobalt-zinc ferrites/graphene nanocomposite. Results Phys. 107576.

Alem, A.F., Worku, A.K., Ayele, D.W., Habtu, N.G., Ambaw, M.D., Yemata, T.A., 2023. Enhancing pseudocapacitive properties of cobalt oxide hierarchical nanostructures via iron doping. Heliyon 9 (3).

Ankita, A., et al., 2024. Europium-doped cerium oxide nanoparticles: investigating oxygen vacancies and their role in enhanced photocatalytic and magnetic properties. Environ. Sci. Pollut. Res. 31 (1), 1276–1287.

Behzad, H., Ghodsi, F.E., 2016. Effect of Zn content on the structural, optical, electrical and supercapacitive properties of sol–gel derived ZnCo2O4 nanostructured thin films. J. Mater. Sci. Mater. Electron. 27, 6096–6107.

Bhargava, R., Khan, S., Ahmad, N., Ansari, M. M. N., 2018, May. Investigation of structural, optical and electrical properties of Co3O4 nanoparticles. In AIP conference proceedings (Vol. 1953, No. 1). AIP Publishing.

Callegari, A., Tonti, D., Chergui, M., 2003. Photochemically grown silver nanoparticles with wavelength-controlled size and shape. Nano Lett. 3 (11), 1565–1568.

Gahrouei, Z.E., Labbaf, S., Kermanpur, A., 2020. Cobalt doped magnetite nanoparticles: synthesis, characterization, optimization and suitability evaluations for magnetic hyperthermia applications. Physica E 116, 113759.

Hafeez, M., Shaheen, R., Akram, B., Haq, S., Mahsud, S., Ali, S., Khan, R.T., 2020. Green synthesis of cobalt oxide nanoparticles for potential biological applications. Mater. Res. Express 7 (2), 025019.

Ibrahim, E.M.M., Abdel-Rahman, L.H., Abu-Dief, A.M., Elshafaie, A., Hamdan, S.K., Ahmed, A.M., 2018. Electric, thermoelectric and magnetic characterization of γ-Fe2O3 and Co3O4 nanoparticles synthesized by facile thermal decomposition of metal-Schiff base complexes. Mater. Res. Bull. 99, 103–108.

Jiangjiang, L., Tian, B., Lu, N., Liu, Z., Zhang, Z., Shi, M., Jiang, Z., 2024. Study on aluminium oxide doping modification of indium oxide and thermoelectric properties. Ceramics Int.

Jincy, C.S., Meena, P., 2022. Evaluation of cytotoxic activity of Fe doped cobalt oxide nanoparticles. J. Trace Elem. Med Biol. 70, 126916.

Karthikeyan, A., Mariappan, R., Bakkiyaraj, R., Santhosh, S., 2023. Comprehensive characterization and electrochemical performance of Fe-doped Co3O4 nanoparticles for energy storage applications. Ionics 29 (12), 5039–5053.

Li, S., Wang, Y., Sun, J., Zhang, Y., Xu, C., Chen, H., 2020. Hydrothermal synthesis of Fe-doped Co3O4 urchin-like microstructures with superior electrochemical performances. J. Alloy. Compd. 821, 153507.

Li, N., Zhao, P., Astruc, D., 2014. Anisotropic gold nanoparticles: synthesis, properties, applications, and toxicity. Angew. Chem. Int. Ed. 53 (7), 1756–1789.

Mahmood, A., Munir, T., Fakhar-e-Alam, M., Atif, M., Shahzad, K., Alimgeer, K.S., Ahmad, S., 2022. Analyses of structural and electrical properties of aluminium doped ZnO-NPs by experimental and mathematical approaches. J. King Saud Univ.-Sci. 34 (2), 101796.

Mahmood, A., Munir, T., Rasul, A., Ghfar, A.A., Mumtaz, S., 2023. Polyethylene glycol and chitosan functionalized manganese oxide nanoparticles for antimicrobial and anticancer activities. J. Colloid Interface Sci. 648, 907–915.

Manickam, M., Ponnuswamy, V., Sankar, C., Suresh, R., Mariappan, R., Chandra Bose, A., Chandrasekaran, J., 2017. Structural, optical, electrical and electrochemical properties of Fe: Co 3 O 4 thin films for supercapacitor applications. J. Mater. Sci. Mater. Electron. 28, 18951–18965.

Munir, T., Mahmood, A., Ahmad, N., Atif, M., Alimgeer, K.S., Fatehmulla, A., Ahmad, H., 2021. Structural, electrical and optical properties of Zn1−xCuxO (x=0.00–0.09) nanoparticles. J. King Saud Univ.-Sci. 33 (2), 101330.

Munir, T., Mahmood, A., Fatima, S., Sohail, A., Fakhar-e-Alam, M., Atif, M., Rafaqat, N., 2023. Structural, optical and thermoelectric properties of (Al and Zn) doped Co9S8-NPs synthesized via co-precipitation method. J. King Saud Univ.-Sci. 35 (7), 102836.

Pagar, T., et al., 2019. "A review on bio-synthesized Co3O4 nanoparticles using plant extracts and their diverse applications. J. Chem. Rev. 1 (4), 260–270.

Sangaiya, P., Jayaprakash, R., 2018. Tuning effect of Sn doping on structural, morphological, optical, electrical and photocatalytic properties of iron oxide nanoparticles. Mater. Sci. Semicond. Process. 85, 40–51.

Soni, A., Maru, M.S., Patel, P., Behal, J., Kaushal, D., Kumar, M., Kumar, S., 2023. Fe-doped nano-cobalt oxide green catalysts for sulfoxidation and photo degradation. Clean Techn. Environ. Policy 1–12.

Stella, C., Soundararajan, N., Ramachandran, K.J.A.A., 2015. Structural, optical, and magnetic properties of Mn and Fe-doped Co3O4 nanoparticles. AIP Adv. 5 (8).

Sun, Z., Liao, T., Dou, Y., Hwang, S.M., Park, M.S., Jiang, L., Dou, S.X., 2014. Generalized self-assembly of scalable two-dimensional transition metal oxide nanosheets. Nat. Commun. 5 (1), 3813.

Xiao, H., Xie, H., Robin, M., Zhao, J., Shao, L., Wei, M., Cui, Z., 2019. Polarity tuning of carbon nanotube transistors by chemical doping for printed flexible complementary metal-oxide semiconductor (CMOS)-like inverters. Carbon 147, 566–573.

Yang, H., Liu, N., Chang, S., Zhao, Y., Liu, Y., 2024. Composite Nanoarchitectonics of Co3O4 Nanopolyhedrons with N-Doped Carbon and Carbon Nanotubes for Alkaline Oxygen Evolution Reaction. Catal. Lett. 1–10.

Yeoh, J.S., Armer, C.F., Lowe, A., 2018. Transition metal oxalates as energy storage materials. A Review. Materials Today Energy 9, 198–222.

Zhang, L., Zhao, X., Ma, W., Wu, M., Qian, N., Lu, W., 2013. Novel three-dimensional Co3 O4 dendritic superstructures: hydrothermal synthesis, formation mechanism and magnetic properties. CrstEngComm 15 (7), 1389–1396.

Zuhra, Z., Ahmad, M., Abbas, Y., Ali, S., Li, S., Hussain, I., Wang, X., 2023. Role of Heteroatoms (N, P, O, and S) in Co3O4-Doped Carbons Derived from ZIF-67-Polyphosphazene Nanohybrids as Anode Materials for Supercapacitors. ACS Appl. Nano Mater. 6 (19), 18045–18053.